REVISTA MATÉRIA V.29 N.3
ISSN 1517-7076 articles e20240244, 2024

Thermal investigation of 12/10 switched reluctance motor adopting different casing fins and materials for e-vehicle application

Karthika Maripandi[1], Balaji Mahadevan[1], Fantin Irudaya Raj Edward Sehar[2], Appadurai Mangalaraj[3]

[1]Sri Sivasubramaniya Nadar College of Engineering, Electrical and Electronics Engineering. Kalavakkam, TN, Índia.

[2]Dr Sivanthi Aditanar College of Engineering, Electrical and Electronics Engineering Tiruchendur. Tiruchendur, Tamilnadu 628215, Índia.

[3]Nehru College of Engineering & Research Centre, Department of Mechanical Engineering. Pampady, Kerala, Índia.

e-mail: karthikam@ssn.edu.in, balajim@ssn.edu.in, fantinraj@gmail.com, appadurai86@gmail.com

ABSTRACT

The current work presents the thermal analysis of a 12/10 switched reluctance motor (SRM) with modified fin arrangements with different materials for e-vehicle applications. Initially, the parameters for the 12/10 SRM were derived using an analytical expression. Electromagnetic analysis was then performed with MagNet software to obtain motor performance metrics such as torque density, ripple, and losses to ensure that the proposed design meets the requirement. Then, a thermal analysis of 12/10 SRM is carried out using Ansys software. Various fin profiles such as conventional rectangular fins, pin fins, thin fins, tapered fins, and tapered slot fins are employed and analyzed to investigate the effectiveness of heat dissipation in motors. The study shows that the tapered slot fin performs better than the other four fin profiles. This is due to its lower mass of 0.53 kg and efficient thermal management (the maximum temperature of the stator outer cover is 31.6 °C). In addition, different fin materials like aluminium (Al), aluminium with 1% graphene particles (GP), and aluminium with 2% GP were analysed for tapered slot fins, and it was found that aluminium with 2% GP provides a lower fin temperature of around 30.40 °C compared to other fin materials.

Keywords: Switched reluctance motor; Casing fins; Fin materials; Electromagnetic analysis; Thermal analysis.

1. INTRODUCTION

Electric vehicles (EVs) are gradually supplanting traditional gasoline-powered vehicles due to their potential to reduce fossil fuel consumption, and climate change, and promote sustainable transportation [1, 2]. For EV's development traction motors play a crucial role. Switched reluctance motors (SRMs) have been adopted for this application solely due to their simplicity, low fabrication cost, high fault tolerance, and ease of cooling [3, 4]. However, SRM has a high-power density, which may result in a high heat load due to small heat dissipation regions, as well as losses such as mechanical, iron, stray, and copper, all of which can raise the temperature of the motor, resulting in high thermal stress, decreased efficiency, and reduced mechanical strength [5–7]. Furthermore, heat from the flow of electric currents and attrition can induce insulation deterioration in the stator, which brings about three to ten per cent of motor failures. Therefore, predicting the temperature rise of an SRM is imperative to its performance. There are numerous methods for examining and calculating a motor's elevated temperature, including analysis with 2-dimensional (2-D) and 3-dimensional (3-D) finite elements. However, calculating the thermal occurrences within an electrical motor is difficult due to a multitude of active thermal exchanges that occur simultaneously. Conduction, radiation, and natural and forced convection, all exist, with their weight per cent varying depending on the motor cooling system, including natural convection, fan, and liquid cooling. Furthermore, multiple thermal sources are operating concurrently. As a result, it is difficult to distinguish between causes and consequences in thermal exchange processes. Therefore, optimizing thermal management and motor cooling systems is essential to increase motor longevity and operational reliability. The literature recommended several cooling techniques and procedures to improve motor performance, such as efficiency and life cycle, because calculating heat generation for cooling is crucial. Furthermore, rising motor temperature significantly reduces performance in terms of output, weight, dimensions, and cost [8–11].

This paper focuses on analysing the electromagnetic and thermal properties of a 12/10 switched reluctance motor for Electric vehicle applications. The electromagnetic study found that the proposed motor meets the

Corresponding Author: M. Karthika Received on 10/05/2024 Accepted on 18/06/2024

DOI: https://doi.org/10.1590/1517-7076-RMAT-2024-0244

Electric vehicle requirement, in addition, different losses were obtained which helped to aid the thermal analysis. Using various fin types and materials thermal analysis was carried out to predict motor temperature, and identify the suitable fins and materials which provide effective heat dissipation, minimal temperature, and less casing weight for Electric-vehicle application.

The manuscript is structured in the following manner: Section 2 included the literature summary of various cooling methods, Section 3 covered the electromagnetic aspects of 12/10 SRM, Section 4 focused on the thermal analysis of 12/10 SRM, Section 5 highlighted the steady state analysis of different fin profiles, Section 6 discussed the findings and discussion, Section 7 provided the effect of different materials on tapered slot fins, and the Section 8 concluded the current and prospective work.

2. LITERATURE SUMMARY

A cooling approach for a 30-KW switched reluctance motor has been developed [12], revealing that liquid water cooling significantly reduces winding temperature by 42% compared to air cooling. The most effective thermal control techniques for the motor's elements have been identified, pinpointing liquid and passive cooling as the finest thermal control techniques [13]. A hybrid cooling system combines air and liquid cooling, including fins on the casing's outside surface, to improve motor safety while preserving thermal insulation [14]. Several cooling systems and calculating procedures for automotive traction motors have been analysed, including forced air, liquid, and natural cooling [15, 16]. A multi-objective optimization technique for a 12/10 switched reluctance motor has been proposed to achieve less temperature, improved torque, and reduced losses [17]. A thermally conductive insert piece for indirect cooling in stator end-windings for a 6/4 switched reluctance motor has been introduced, achieving 26.5 A/mm^2 current density [18]. A lightweight material, temperature-reducing tactics, material changes, coolants, and numerical approaches for permanent magnet synchronous motors have been presented [19, 20]. Sophisticated cooling schemes for Permanent Magnet Synchronous Motor (PMSMs) have been proposed, analysing topologies, thermal design challenges, materials, and performance to provide recommendations for improved motor design and innovative cooling solutions [21]. Thermal modelling and analysis of a 10-KW double-stator SRM have been proposed, analysing temperature distribution, and using water as a coolant via computational fluid dynamics [22].

The thermal and mechanical performance of a 72/48 switched reluctance motor in a low-speed direct-drive mining system was investigated, highlighting that optimizing cooling jacket designs elevates natural frequency while minimizing motor weight and temperature [23]. A magneto-thermal model has been proposed for forecasting the temperature distribution of a switched reluctance motor (SRM) and diagnosing faults [24]. A thermomagnetic system of a 3-KW switched reluctance motor was investigated to improve cooling performance using aluminium fins [25]. An analytical thermal model for winding temperature estimations in symmetrical and asymmetrical currents was proposed, focusing on enhancing motor lifespan in DC charging mode [26]. A sequential adaptive fluid-solid coupling approach was introduced for estimating loss and predicting elevated temperatures in high-speed, high-power switching reluctance machines, which is faster and more efficient than direct coupling methods [27]. A thermal circuit model for a 6/4 switched reluctance motor was also proposed to predict the whole motor temperature during working conditions [28].

The literature addresses numerous cooling approaches, including air, natural, forced, water, and adaptive ways, to promote motor efficiency, safety, and longevity. These strategies contribute to keeping motor temperatures below safe ranges, preventing component deformation, and preventing installation failure, all of which improve efficiency but research lacks of address for ideas of using various fins and different materials for temperature reduction of the switched reluctance motor.

3. ELECTROMAGNETIC EVALUATION OF SIX PHASE SWITCHED RELUCTANCE MOTOR

This section looks at the attributes and electromagnetic response of a six-phase switched reluctance motor (SRM) which is devised for an electric vehicle with a rating of 5-KW output power and torque of 10 Nm. Electromagnetic analysis was performed with MagNet software to validate the model and its performance. The motor consists of 12 stator slots and 10 rotor poles as illustrated in Figure 1. Two coils are sequentially connected to form each phase [29, 30]. The SRM employs the reluctance principle, in which the rotor strives to align excited stator poles, so producing torque. The proposed 12/10 SRM design (12 poles in stator and 10 poles in rotor) offers a high number of phase configurations when compared with the 12/8 SRM design (12 stator poles and 10 rotor poles). The high number of poles in the proposed model provides better results in terms of higher torque and power density and yields minimum torque ripple compared with conventional SRM models [31–33]. The specification details of the 12/10 SRM proposed in the present work are acquired via an analytical equation which is elucidated

in Tables 1 and 2. and its machine length and stator outer and shaft radius, are picked out as per the prescribed power and torque output.

The model's validation and performance assessment involve conducting electromagnetic analysis of 12/10 SRM via finite element-based software for assessing motor performance indicators including torque, ripple, and efficiency, which were identified to establish if the proposed design matches the expectations of an electric vehicle. The motor losses were also found, whereas losses within machine parts are a significant contributor to increased thermal generation.

Figure 1 illustrates the 12/10 SRM is tailored for the specification given in Table 2. The dynamic torque and flux plot of 12/10 SRM is illustrated in Figures 2 and 3. Figure 2 shows that 12/10 SRM generates the above-described torque at a rated current of 110 amps and a speed of 4500 rpm, which can be determined by averaging the torque curves.

Table 1: Mathematical expression for design parameters of switched reluctance motor.

VARIABLES	EXPRESSION
Stator pole surface area (A_s)	$A_s = \frac{D_{BO}}{2} * M_L * B_S$
Stator pole magnetic flux (φ)	$\varphi = B_s * A_s$
Stator yoke magnetic flux (φ_y)	$\varphi_y = \frac{B_{st} * A_s}{2}$
Yoke surface area (A_Y)	$A_Y = A_S$
Stator core thickness (C_T)	$C_T = \frac{A_Y}{L}$
Stator pole length (S_{PL})	$S_{PL} = \frac{D_{SO}}{2} - C_T - \frac{D_{BO}}{2}$
Rotor pole surface area (A_r)	$A_r = \left(\frac{D_{BO}}{2} - G_a\right) M_L B_r$
Rotor core surface area (A_{rc})	$A_{rc} = \frac{A_s}{1.6}$
Rotor pole length (R_{PL})	$R_{PL} = \frac{D_{Bo}}{2} - G_a - \frac{D_{So}}{2} - \frac{A_{rc}}{L}$

Table 2: Specification details of 12/10 SRM.

VARIABLES	VALUES
Rated current	108 amps
Stator outer diameter, D_{SO}	154 mm
Inner diameter of stator, D_{BO}	84 mm
Machine length, M_L	150 mm
Stator pole length, S_{PL}	23 mm
Stator pole span, S_{PS}	12 degrees
Rotor pole length, R_{PL}	18.5 mm
Rotor pole span, R_{PS}	18 degrees
Shaft diameter, S_D	19 mm

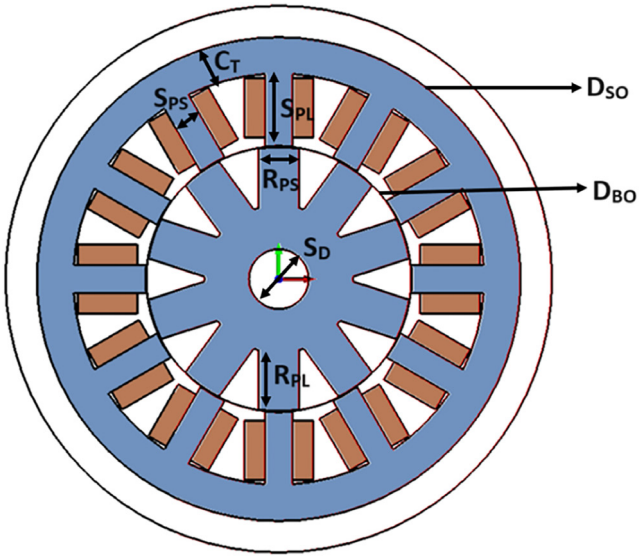

Figure 1: Structural layout of 12/10 switched reluctance motor.

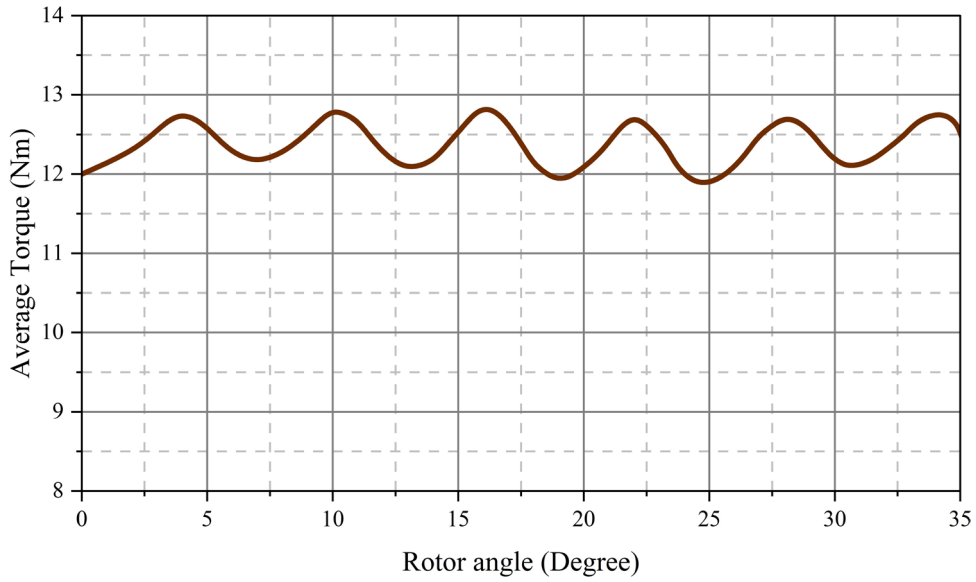

Figure 2: Dynamic torque vs rotor angle of 12/10 SRM.

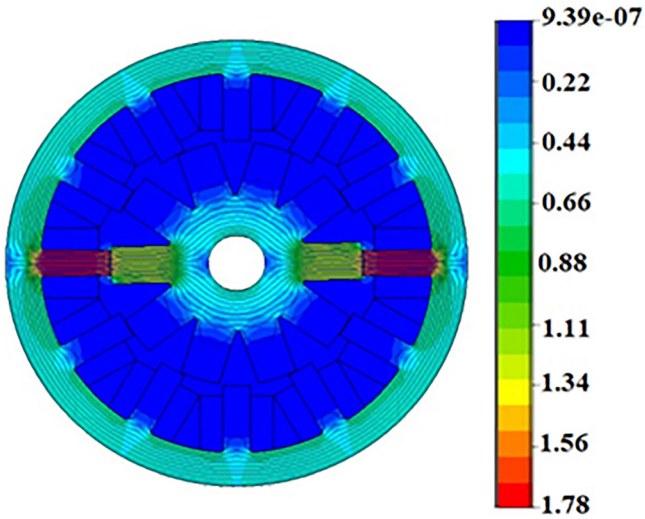

Figure 3: Flux line dispersal pattern of 12/10 SRM.

Analysing the flux density plot has significance for motor design because it provides insights into the distribution and interaction of magnetic flux within the stator and rotor core, which influences motor torque and speed characteristics. The torque generated by the motor is proportional to the magnetic flux density in the air gap between the stator and rotor and it is also beneficial to monitor leakage flux distribution to avoid performance degradation due to increased losses [34].

Table 3: Performance metrics of 12/10 SRM.

VARIABLES	OUTPUT
Torque	12.42 Nm
Torque ripple	0.08 p.u.
Efficiency	93.22%
RMS current density	6.5 A/mm^2
Torque per unit rotor volume (TRV)	14.95 KNm/m^3
Loss - Winding	0.21 KW
Total loss	0.423 KW

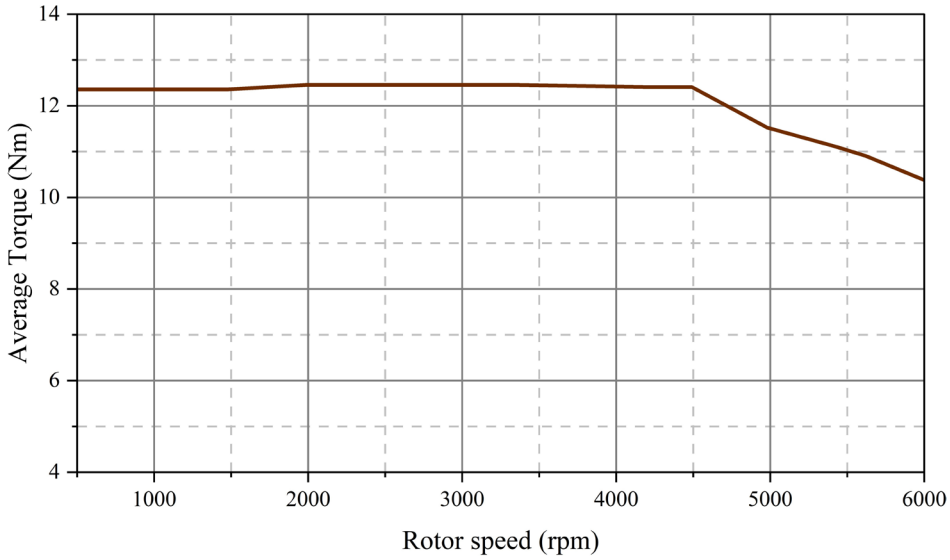

Figure 4: Torque vs speed plot of 12/10 SRM.

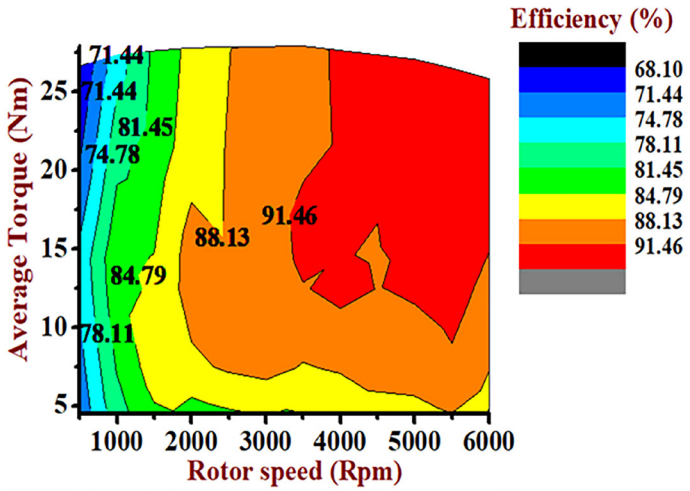

Figure 5: Efficiency plot of 12/10 SRM.

The flux density map helps to assess whether the developed magnetic flux can generate the required torque of the motor at the rated current. It also aids in design validation and optimization of the motor by identifying saturation points in the motor magnetic core, and ensuring that the saturation level is within the limit of magnetic material, to prevent thermal issues like overheating or insulation breakdown for implementing better cooling strategies to maintain the optimal motor performance and its longevity.

Figure 3 reflects the flux pattern of 12/10 SRM, with maximum flux prevailing during the aligned state of poles at the rated current of 110 amps. Here, the materials used for the analysis is M-19 silicon steel. The results show that the design achieves a maximum flux of 1.78 T, which does not exceed the saturation threshold of M-19 material.

The results in Table 3 show that 12/10 SRM designs are capable of yielding the necessary average torque, torque per unit volume, as well as reduced torque ripple, improved efficiency, and rms current density that remains within limits. The layout is further examined to determine this design complies with the standards for electric vehicle specifications. The Figures 4 and 5 displays the torque speed and efficiency plot of 12/10 SRM.

The torque-to-speed plot of 12/10 SRM are shown in the charts above. As shown in this preceding figure, it provides the appropriate torque up to the nominal speed of 4500 rpm then stabilizing once it's exceeded its top speed.

The motor's performance is examined using an efficiency map. The diagram depicts efficiency at various operating points. In this investigation, the motor speed is ranged from 0 to 6000 rpm, while the load is ranged from 0 to 25 Nm.

The efficiency at every single operating point has been determined using the preceding given Figure 5. The devised efficiency map displays that SRM performs better at its nominal speed with a torque of 10 Nm at 4500 rpm, and at top speed with a torque of 26 Nm at 6000 rpm, and it provides excellent efficiency of about 91%, as seen in the figure. The primary advantage of the proposed SRM is it delivers excellent efficiency in flux-weakening zones.

4. TRANSIENT THERMAL ANALYSIS OF 12/10 SRM

A simplified 3-D geometrical model of the electric motor is created is shown in Figure 6, which represents the conventional motor's geometry and its meshing geometry is Figure 7.

The electric motor is dominant equipment in all engineering applications due to its compact and simple construction. The motor consumes a larger ampere of current at the starting condition to attain the rated speed. The initial torque is high and it is in a steady state. The electric motor's parameters continuously vary up to the rated speed. The heat energy induced inside the motor are also high due to this condition. For understand the heat dissipation at the initial condition the transient analysis is done in the ANSYS workbench.

Figure 8 shows the thermal contour of the motor in a transient state. The maximum temperature in the stator is found to be 46.128 °C. The proper fin profile is required for the dissipation of induced thermal energy to the surroundings for the minimal temperature inside the motor.

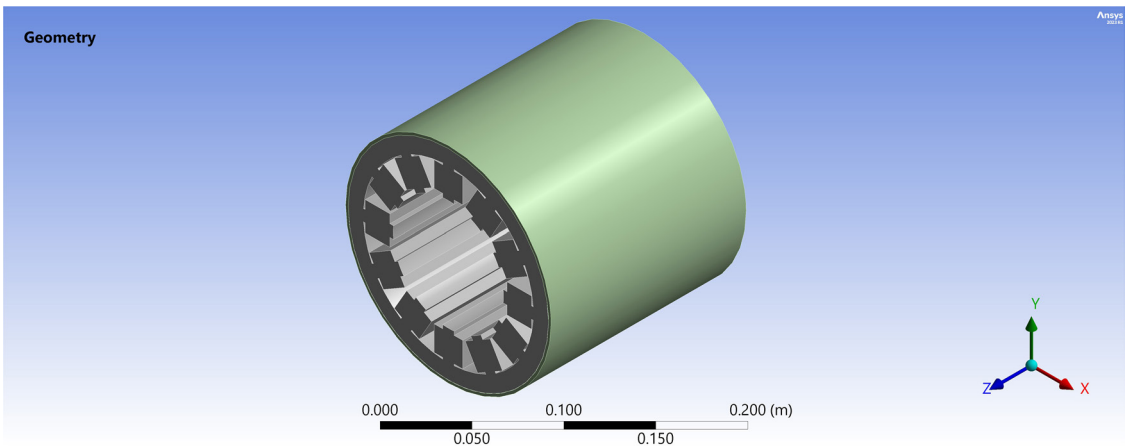

Figure 6: CAD model of 12/10 SRM.

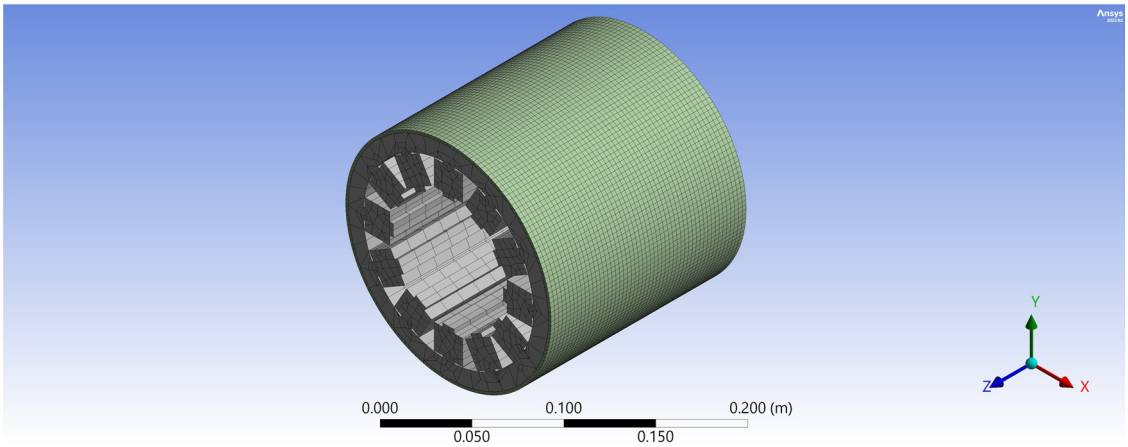

Figure 7: Meshing of 12/10 SRM.

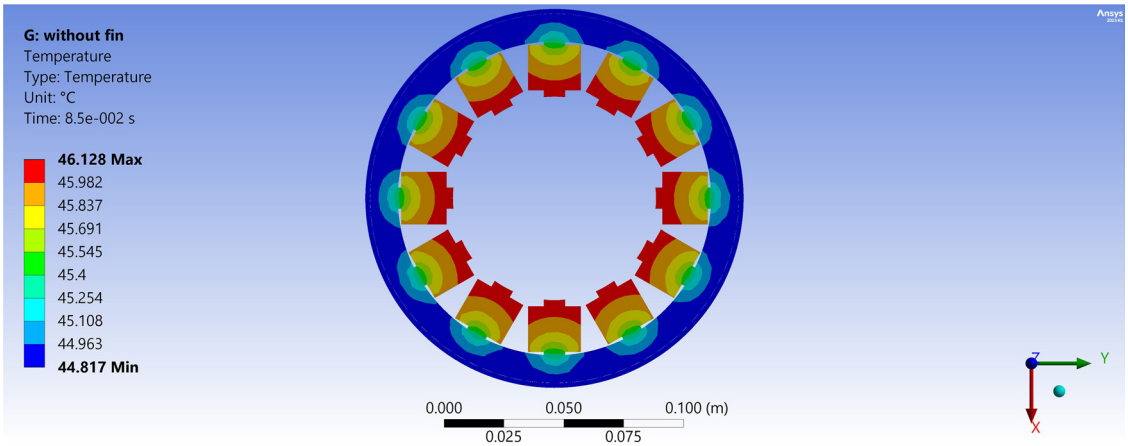

Figure 8: Distribution of temperature during transient analysis of 12/10 SRM.

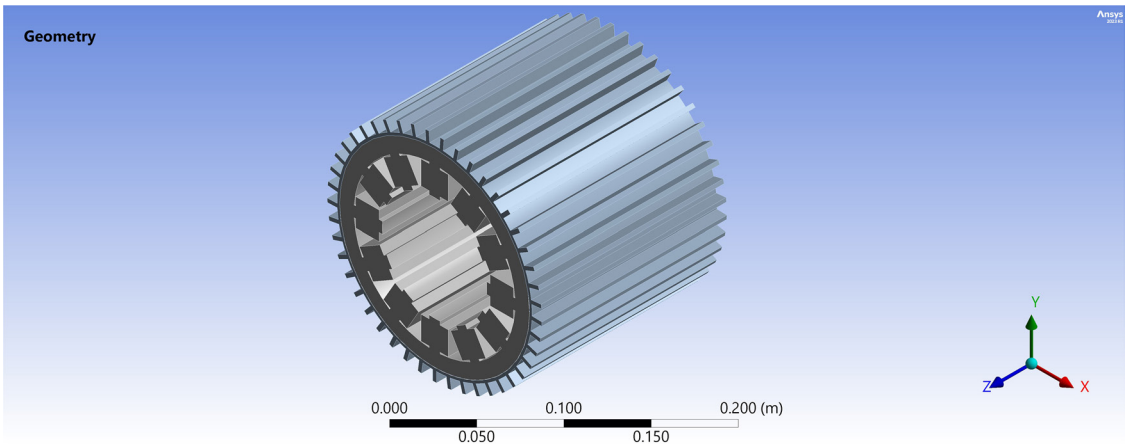

Figure 9: 12/10 SRM with conventional rectangular fin casing.

5. STEADY-STATE ANALYSIS OF DIFFERENT FIN PROFILE

The electric motor stator is generally made of silicon steel and the casing with fins is made of aluminium. The aluminium material has higher thermal conductivity, low cost and workability. The effect of fins on inducted heat dissipation can be understood from the steady state analysis.

Here, five types of fins namely conventional rectangular fin (Figure 9), pin fin (Figure 10), thin fin (Figure 11), tapered fin (Figure 12) and tapered slot fin (Figure 13) are chosen for numerical simulation. The results of different fin profiles are compared to opt out of the suitable fin profile for electric motors which is

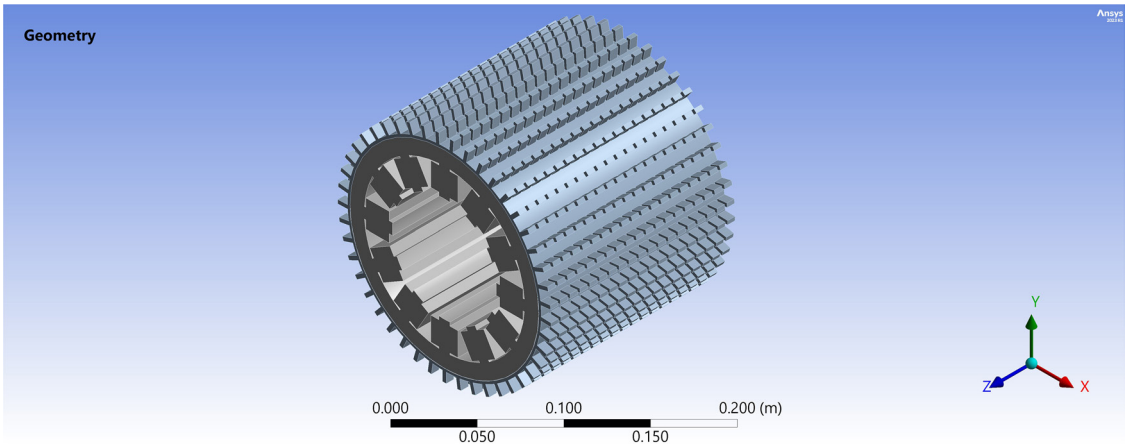

Figure 10: 12/10 SRM with pin fin casing.

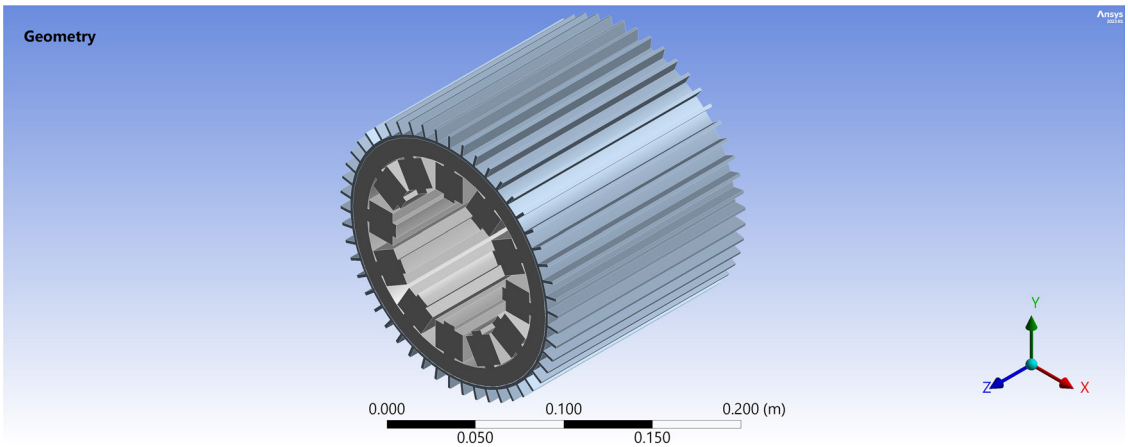

Figure 11: 12/10 SRM with thin fin casing.

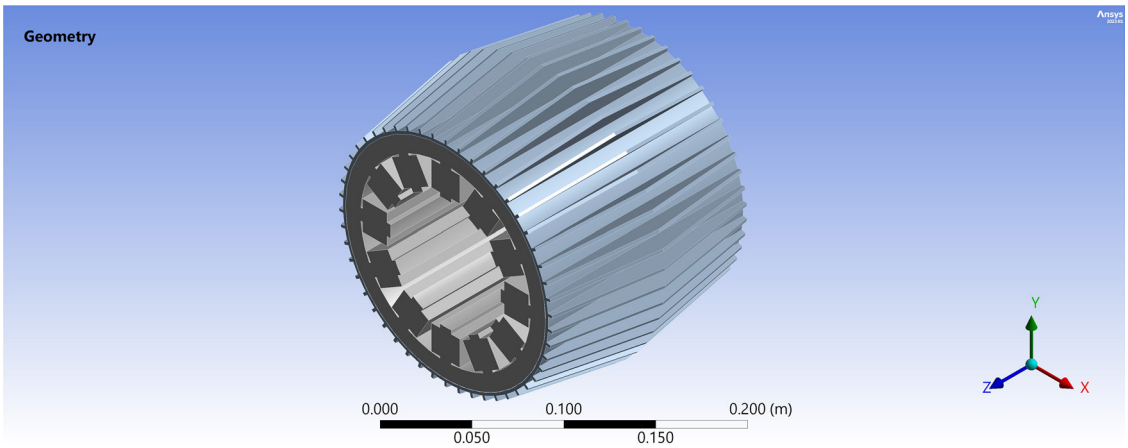

Figure 12: 12/10 SRM with tapered fin casing.

utilized in several engineering fields. All simulations are conducted using the steady-state thermal module in ANSYS Workbench, with the steps detailed for each case.

5.1. Meshing of different fin profile

To ensure accurate numerical simulation, a high-quality mesh is required. After importing the CAD model, a mesh is generated and thoroughly evaluated using a grid independence test before applying boundary conditions. Table 4 presents the optimum number of elements; and node count of discretized geometry. These values

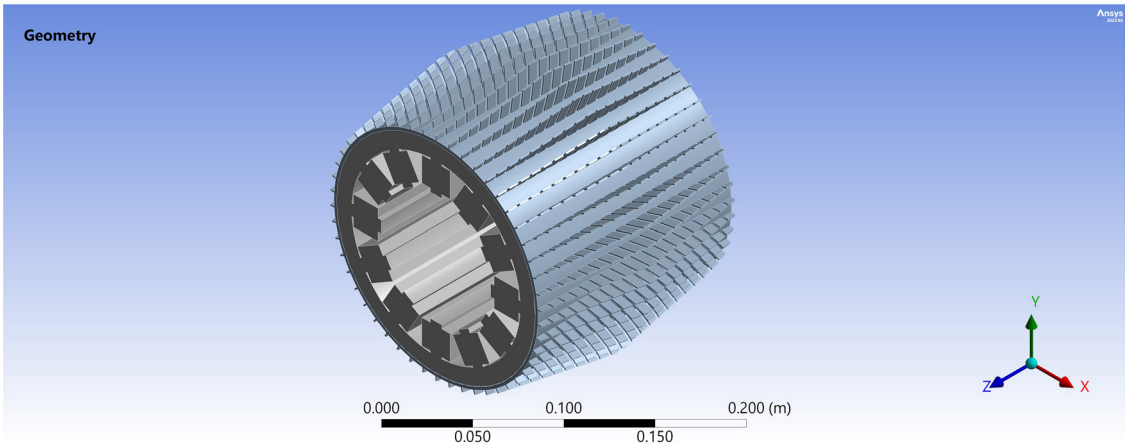

Figure 13: 12/10 SRM with tapered slot fin casting.

Table 4: Optimum element and nodes count.

FIN GEOMETRY	NO. OF ELEMENTS	NO. OF NODES
1	147799	194820
2	190122	51048
3	564337	918490
4	746851	137837
5	1679057	440504

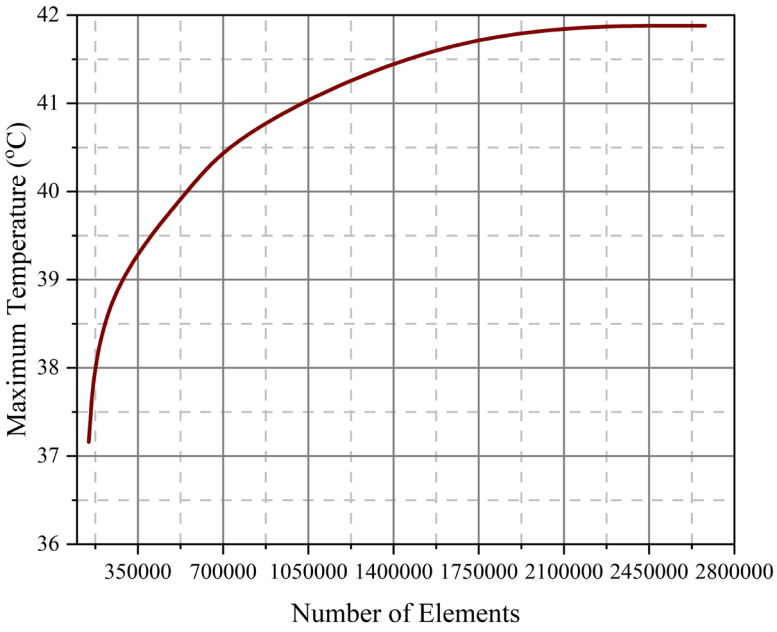

Figure 14: Discretization study.

are obtained from the ANSYS software post-meshing, which serves as indicators of mesh quality. Figure 14 represents the discretization study of the CAD model. From discretization study, the optimum element count can be obtained. The value of the temperature is not changing after the certain number of elements counts. That grid can be used in the numerical analysis. Figures 15 to 19 depict the grids generated for all fin geometries.

5.2. Numerical simulations

The numerical simulation solves governing equations, which can represent steady or unsteady. For this numerical simulation, steady-state analysis is conducted. Electric motor contours of temperature distribution

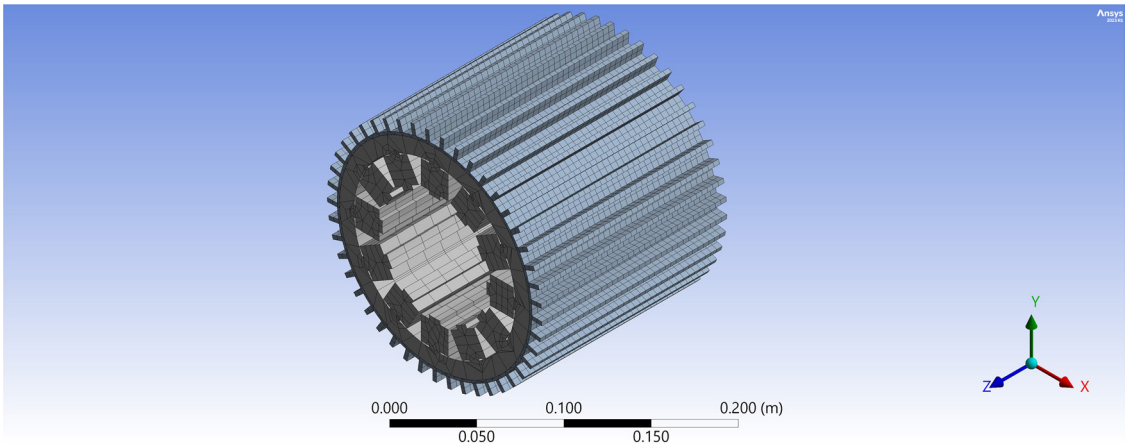

Figure 15: Meshing of 12/10 SRM with conventional rectangular fin.

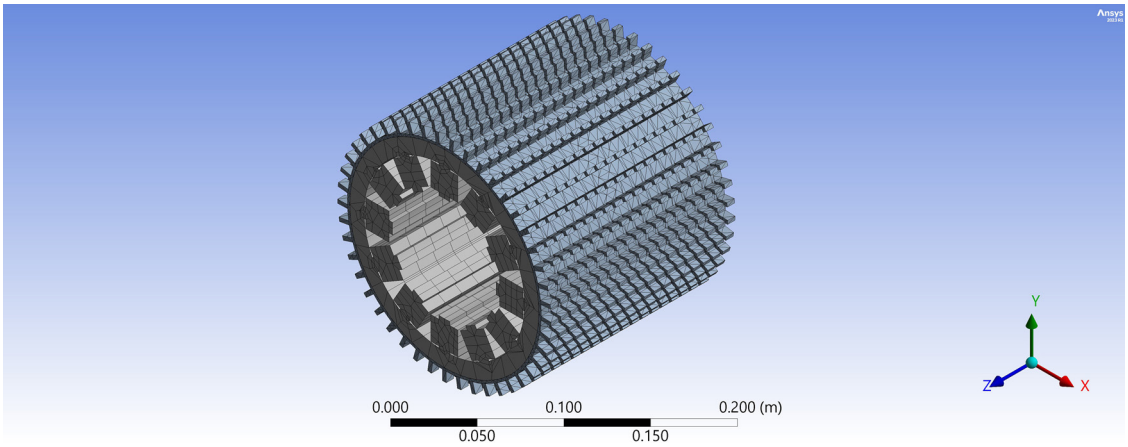

Figure 16: Meshing of 12/10 SRM with pin fin.

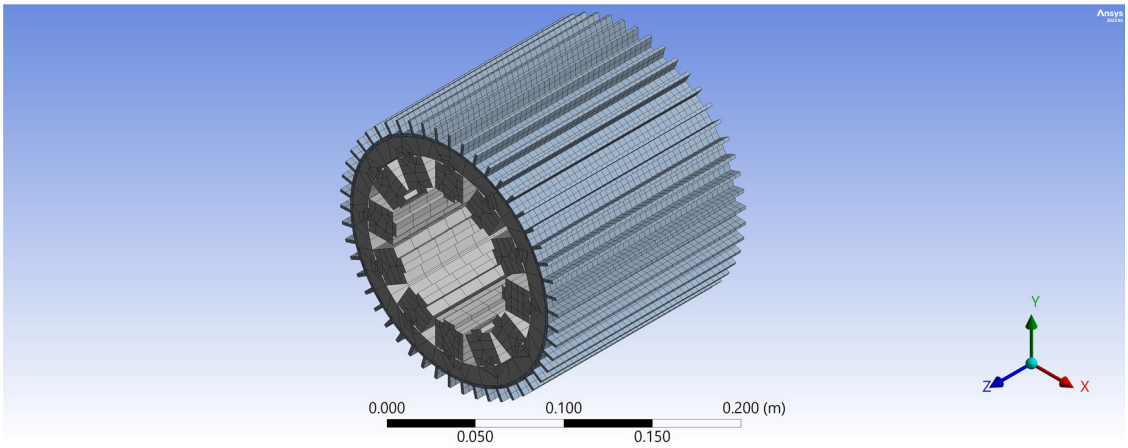

Figure 17: Meshing of 12/10 SRM thin fin.

are obtained by selecting the contour option in the post-processing window. Additionally, maximum, minimum, and average temperature values are extracted from the contour details. The numerical values at each of the contours are generated by selecting the required area and plotting it. After getting the numerical values from the simulation, the graphs are drawn to compare the effect of different fin profiles for further discussion on the obtained results.

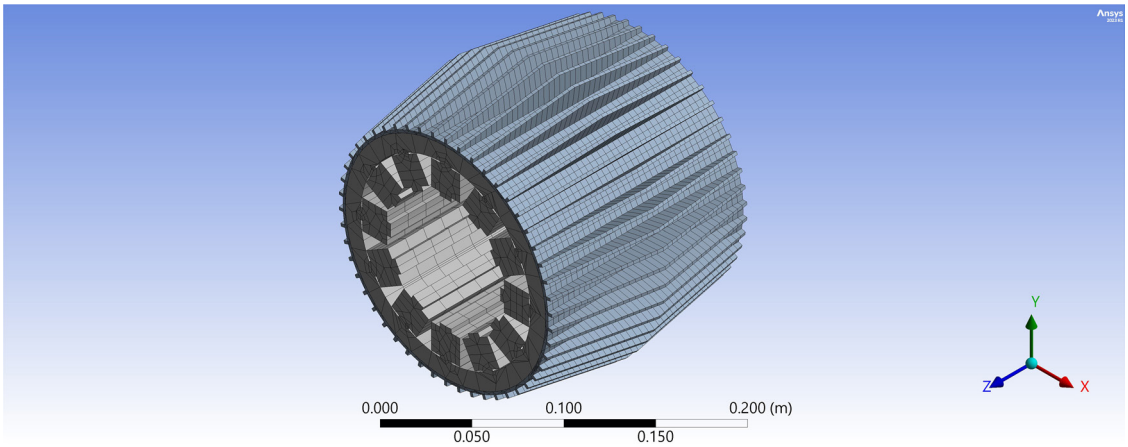

Figure 18: Meshing of 12/10 SRM with tapered fin.

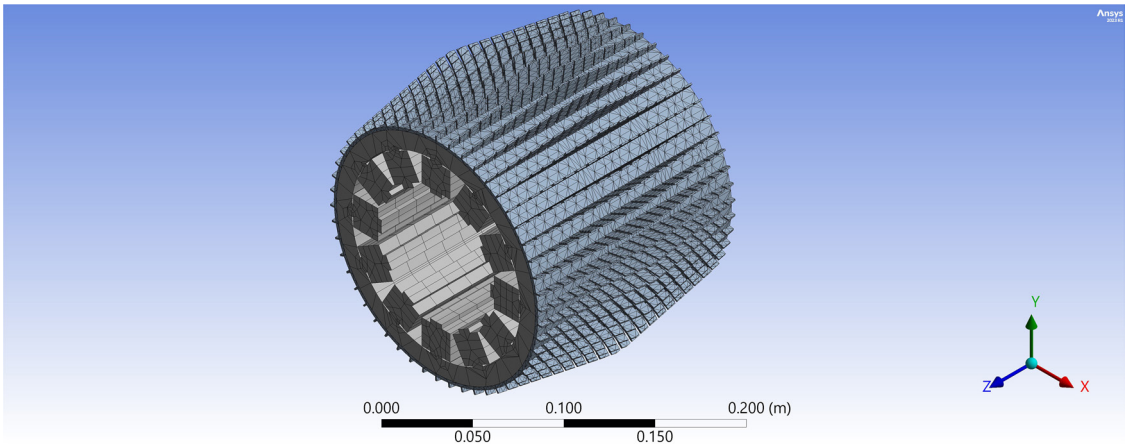

Figure 19: Meshing of 12/10 SRM with tapered slot fin.

6. RESULTS AND DISCUSSION

Several types of fins are proposed in this manuscript. The numerical analysis is done for all types of fins to investigate the effectiveness of heat dissipation from the electric motor. The minimum temperature at the motor surface is concluded as effective fin geometry. Since the proper heat dissipation from the electric motor surface leads to the minimal temperature around it. The other factor which decides the choice of fin type is its mass. The engineering applications required less-weight objects. After the numerical analysis, these two factors such as minimal temperature at the motor surface and less weight are noted from the simulation results, the best type of fin geometry will be concluded among all other types of fins.

6.1. 12/10 SRM with conventional rectangular fin

The conventional fin is well known for its simple design. Due to its simple design, these fins are highly flexible for casting. Here 40 fins are distributed on the circumference of the motor and the fin thickness is 3 mm. The thermal energy dissipation of the casing with conventional rectangular fin, obtained from the ANSYS solver is shown in Figure 20. The fin geometry weight is 0.8368 kg. The temperature at the fin surface is 39.329 °C.

6.2. 12/10 SRM with pin fin

The familiar fin profile used in engineering applications is the pin fin is shown in Figure 21. The pin fins are just extruded from the base surfaces to augment the heat transfer rate. This type of fin is designed by making parallel slots across the rectangular fins to reduce its weight. Several types of pin fin are commercially available, of these rectangular fins have good thermal performance and are reliable to manufacture. The maximum fin tip temperature is 36.199 °C and the casing weight is 0.73148 kg.

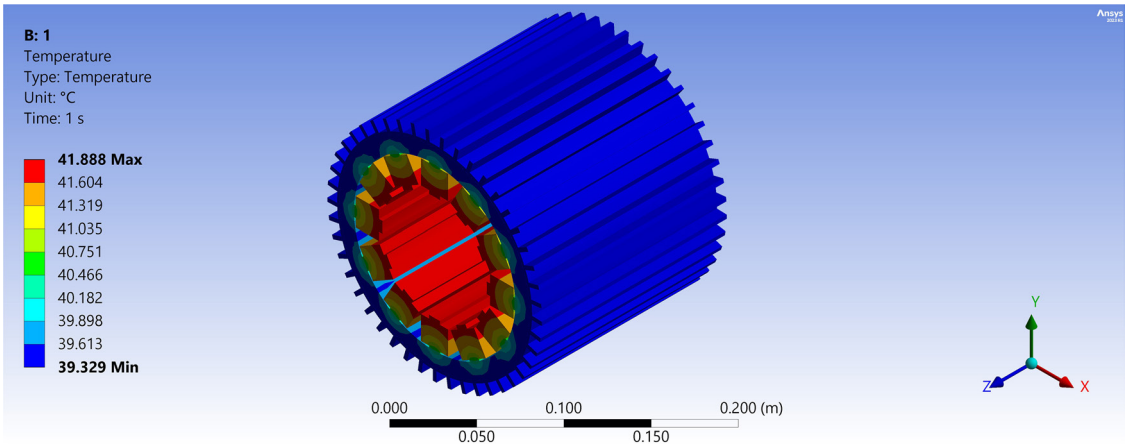

Figure 20: Temperature profile of 12/10 SRM with conventional rectangular fin casing.

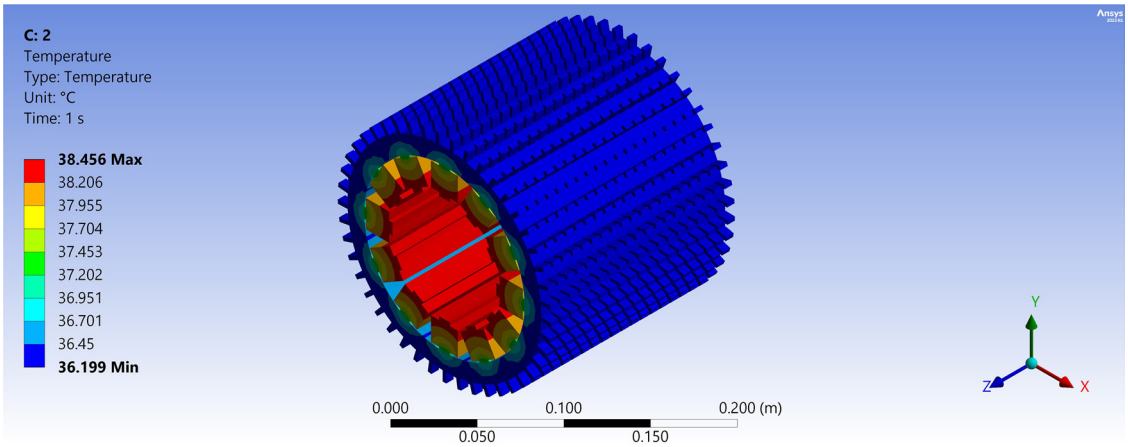

Figure 21: Temperature profile of 12/10 SRM with pin fin.

6.3. 12/10 SRM with thin fin

The convective heat transfer is proportional to the surface area of the fin profile. The thin fins have larger surface area exposed to the surroundings. Several types of heat exchangers utilise this type of fin profile. The number of fins is higher in this type of fin profile. Here 50 fins are distributed around the circumference of the motor and its thickness is 1 mm. The temperature profile of the motor casing with thin fin is shown in Figure 22. The maximum fin tip temperature is 35.565 °C and the casing weight is 0.72293 kg. The maximum fin tip temperature of thin fin is very minimal, when compared to conventional fin because of its larger surface area.

6.4. 12/10 SRM with tapered fin

The electric rotor continuously runs due to the repulsion between the two magnetic fields. Here the major fraction of electrical energy is converted into mechanical energy and the remaining is dissipated as heat to the surroundings. The generated heat must be released into the environment for the efficient performance of the electric motor. In this type of fin, at the centre, the fin height is larger and gradually decreases towards the side of the electric. Since the generated heat at the centre is released to the surroundings through the stator sideways or through fin. The maximum fin height at the centre augments the heat losses through the fin surfaces is given in Figure 23. The maximum fin tip temperature is 33.507 °C and the casing weight is 0.76938 kg.

6.5. 12/10 SRM with tapered slot fin

In this type of fin, the parallel slot cuts are made on the taper fin as illustrated in Figure 24. This enhances the surface area of the fin exposed to the ambient air and reduces its weight. The casing weight is 0.5379 kg,

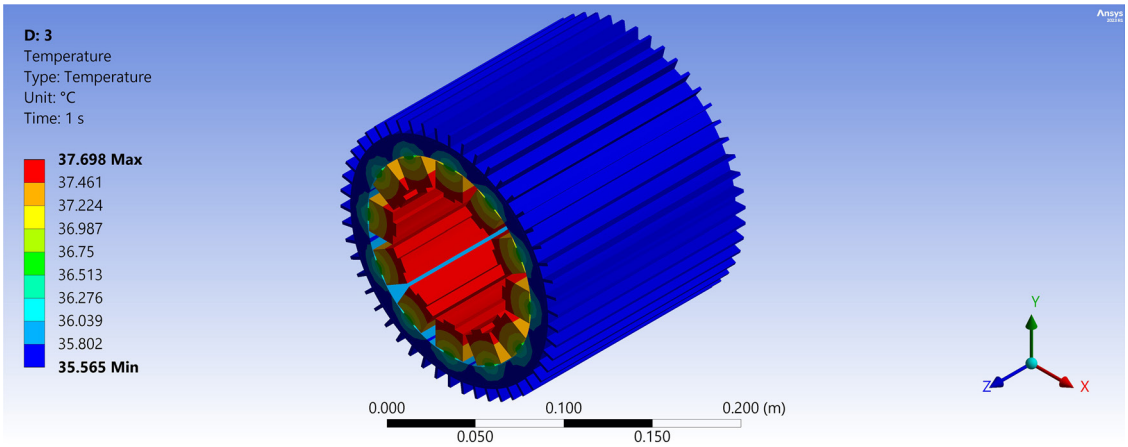

Figure 22: Temperature profile of 12/10 SRM with thin fin.

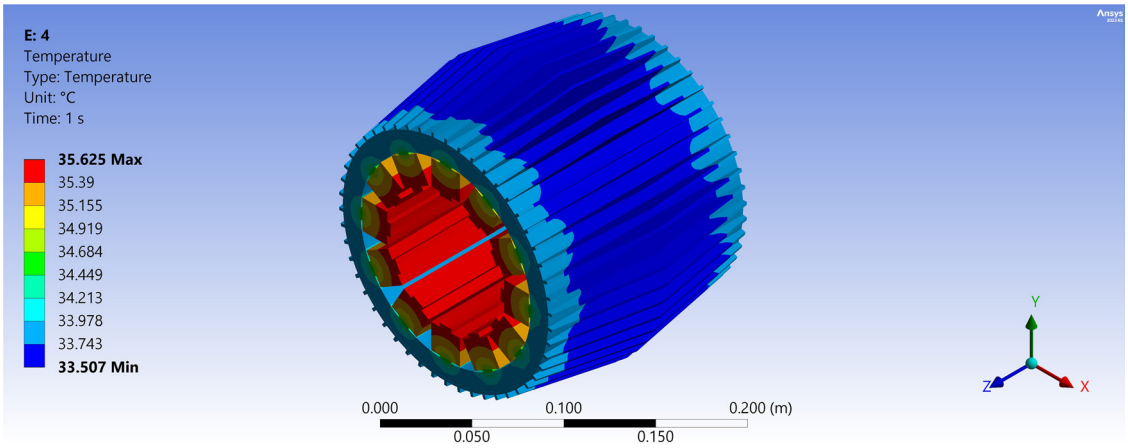

Figure 23: Temperature profile of 12/10 SRM with tapered fin.

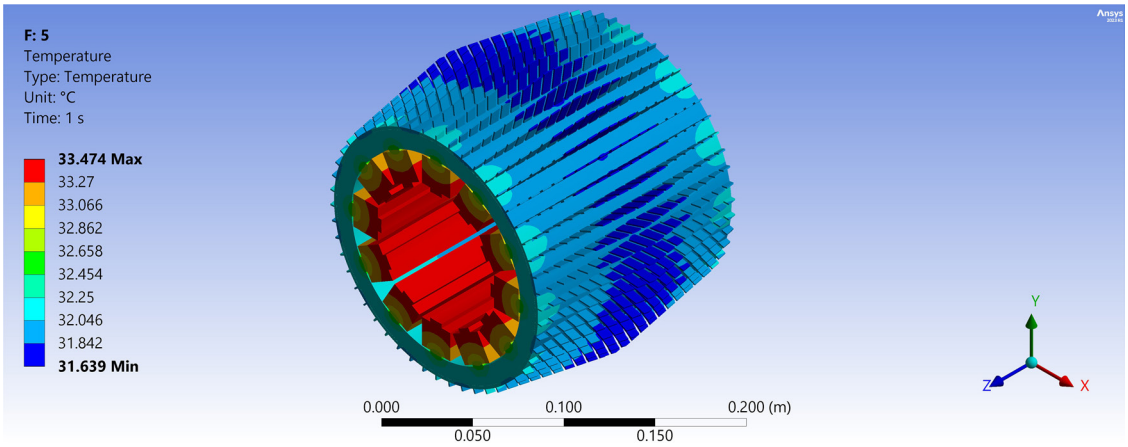

Figure 24: Temperature profile of 12/10 SRM with tapered slot fin.

which is very minimal compared to other types of fins. This type of fin shows better performance because of its enhanced surface area. The fin tip maximum temperature is 31.639 °C, which is also less in comparison with the remaining fin types. Table 5, elucidates the comparison of different fin profiles for 12/10 SRM and its associated outcomes of temperature and mass.

From Figure 25, the tapered slot fin shows better results, when compared to the remaining four fin profiles. Since the mass of the tapered slot fin is less as well as the stator maximum temperature is also

Table 5: Comparison of different fin profiles.

DIFFERENT FIN PROFILE	FIN TIP TEMPERATURE (°C)	MASS (kg)
12/10 SRM with conventional rectangular fin	39.329	0.8368
12/10 SRM with pin fin	36.199	0.73148
12/10 SRM with thin fin	35.565	0.72293
12/10 SRM with tapered fin	33.507	0.73938
12/10 SRM with tapered slot fin	31.639	0.5379

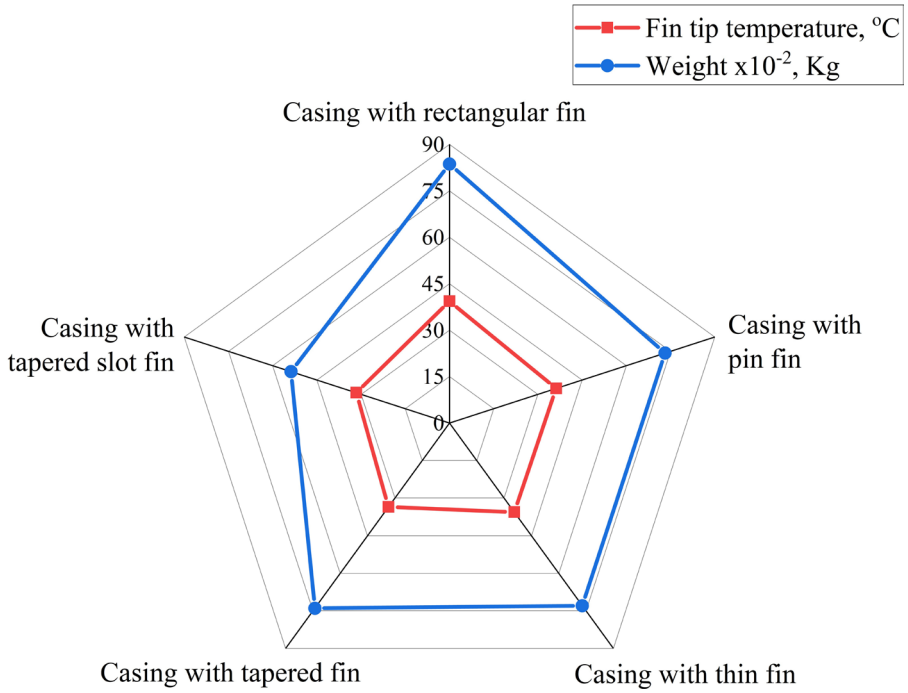

Figure 25: Comparison of maximum fin tip temperature and weight of different fin profiles.

Table 6: Thermal properties of fin materials.

MATERIALS	THERMAL CONDUCTIVITY (K) w/m k	DENSITY (ρ) kg/m³
Aluminium (Al)	220	2700
Al with 1% GP [35]	280	2695
Al with 2% GP [35]	312.5	2675
M19 [36]	21.9	7450

found to be less. Here the aluminium is chosen for the numerical study. Further, the effect of different aluminium metal matrix composite materials on heat energy dissipation is studied through numerical analysis.

7. EFFECT OF DIFFERENT MATERIALS ON TAPERED SLOT FIN

Aluminium is a good thermal conductor and is more economical. Most applications utilized aluminium as a thermal conductor. The thermal conductivity of aluminium is further improved by adding high thermal conductivity materials as metal matrix. Here, graphene metal matrix is chosen for numerical simulation.

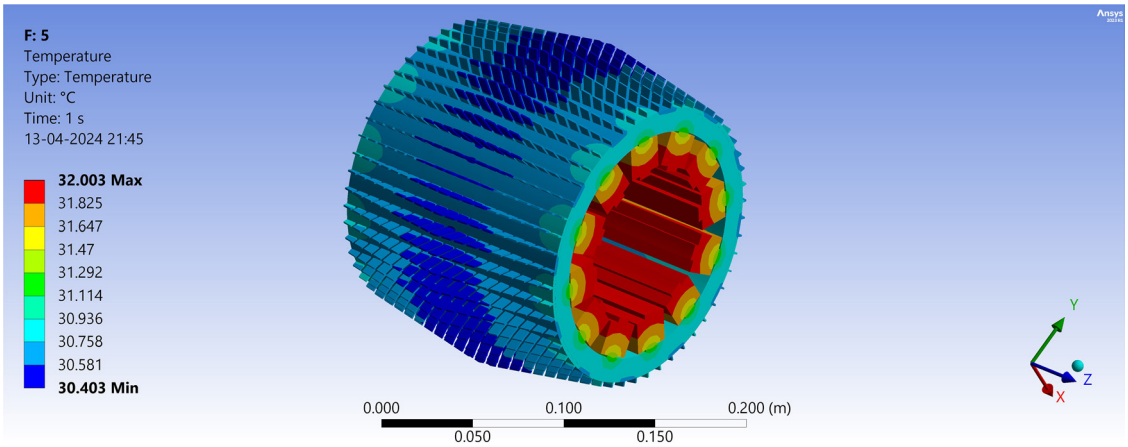

Figure 26: Temperature profile of fin made of Al 2% GP.

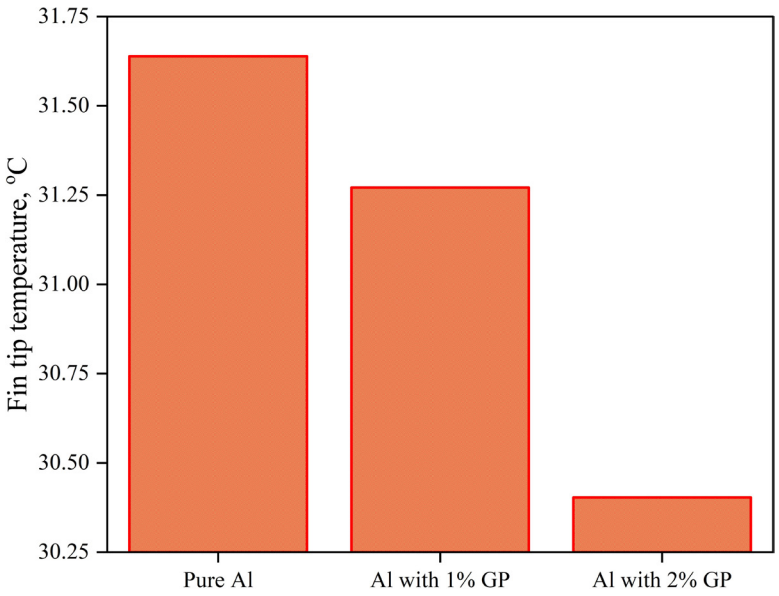

Figure 27: Comparison of fin tip temperature.

Two MMCs namely Al with 1% and 2% weight graphene particles (GP). The numerical study is made in the ANSYS software and the results of Al with 2% GP fin are shown in Figure 26. Other simulation results are compared in Figure 27. The surface temperature of fin is found to be 30.403 °C and the inside stator temperature is 32.003 °C. The simulation results revealed that Al with 2% has better performance when compared with other fin materials as cleared in Table 6 and Figures 26 and 27.

8. CONCLUSION

In this manuscript, the comprehensive thermal analysis of a 12/10 switched reluctance motor (SRM) which is suitable for electric vehicle applications is presented. Initially, the design parameters were derived analytically, and the model's performance was validated through electromagnetic analysis using MagNet software. The key motor performance metrics such as torque density, ripple, and losses were examined to ensure suitability across various engineering applications. Further, the thermal analysis was conducted using ANSYS software. The several types of fin profiles were analysed in ANSYS to study their effectiveness. The numerical analysis results indicate that the tapered slot fins exhibit superior performance compared to conventional rectangular, pin, thin, and tapered fins, which had a lower mass of 0.53 kg and stator maximum temperature of 31.6 °C. The different fin materials namely aluminium with 1% GP and aluminium with 2% GP were proposed for the tapered slot fins. The numerical analysis of various fin materials showed that the aluminium with 2% GP had the lowest fin temperature of 30.403 °C, surpassing other material options.

9. BIBLIOGRAPHY

[1] DIAO, K., SUN, X., LEI, G., *et al.,* "Multimode optimization of switched reluctance machines in hybrid electric vehicles"*, IEEE Transactions on Energy Conversion***,** v. 36, n. 3, pp. 2217–2226, 2020. doi: http://doi.org/10.1109/TEC.2020.3046721.

[2] RAJ, E.F.I., APPADURAI, M., RANI, E.F.I., *et al*., "Finite-element design and analysis of switched reluctance motor for automobile applications", *Multiscale and Multidisciplinary Modeling, Experiments and Design*, v. 5, n. 3, pp. 269–277, 2022. doi: http://doi.org/10.1007/s41939-022-00119-8.

[3] YAN, W., CHEN, H., LIAO, S., *et al*., "Design of a low-ripple double-modular-stator switched reluctance machine for electric vehicle applications", *IEEE Transactions on Transportation Electrification*, v. 7, n. 3, pp. 1349–1358, 2021. doi: http://doi.org/10.1109/TTE.2021.3057133.

[4] SIJINI, A.C., FANTIN, E., RANJIT, L.P., "Switched reluctance motor for hybrid electric vehicle", *Middle East Journal of Scientific Research*, v. 24, n. 3, pp. 734–739, 2016.

[5] HAN, S., DIAO, K., SUN, X., "Overview of multi-phase switched reluctance motor drives for electric vehicles", *Advances in Mechanical Engineering*, v. 13, n. 9, pp. 16878140211045195, 2021. doi: http://doi.org/10.1177/16878140211045195.

[6] AUGUSTINE, M., RAJ, E.F.I., APPADURAI, M., *et al*., "Impact of silicon steel laminating materials in segmented rotor switched reluctance motor: electromagnetic and vibrational analysis", *Journal of Vibration Engineering & Technologies*, v. 12, n. 3, pp. 3931–3946, 2024. doi: http://doi.org/10.1007/s42417-023-01097-y.

[7] INFANTRAJ, A., AUGUSTINE, M., RAJ, E.F.I., *et al*., "Investigation of various laminating materials for interior permanent magnet brushless DC motor for cooling fan application", *CES Transactions on Electrical Machines and System*s, v. 7, n. 4, pp. 422–429, 2023. http://doi.org/10.30941/CESTEMS.2023.00048.

[8] FAIZ, J., GANJI, B., CARSTENSEN, C.E., *et al*., "Temperature rise analysis of switched reluctance motors due to electromagnetic losses", *IEEE Transactions on Magnetics*, v. 45, n. 7, pp. 2927–2934, 2009. doi: http://doi.org/10.1109/TMAG.2009.2015755.

[9] XU, Z., XU, Y., GAI, Y., *et al*., "Thermal management of drive motor for transportation: analysis methods, key factors in thermal analysis, and cooling methods: a review", *IEEE Transactions on Transportation Electrification*, v. 9, n. 3, pp. 4751–4774, 2023. doi: http://doi.org/10.1109/TTE.2023.3244907.

[10] APPADURAI, M., RAJ, E.F.I., RAM, V., *et al*., "Investigation of solar air collectors with carbon-nanotube-based turbulators and pin fin arrangements", *Journal of Composites Science*, v. 7, n. 8, pp. 322, 2023. doi: http://doi.org/10.3390/jcs7080322.

[11] FANTIN IRUDAYA RAJ, E., BALAJI, M., "Analysis and classification of faults in switched reluctance motors using deep learning neural networks", *Arabian Journal for Science and Engineering*, v. 46, n. 2, pp. 1313–1332, 2021. doi: http://doi.org/10.1007/s13369-020-05051-y.

[12] CHIU, H.C., JANG, J.H., YAN, W.M., *et al*., "Thermal performance analysis of a 30 kW switched reluctance motor", *International Journal of Heat and Mass Transfer*, v. 114, pp. 145–154, 2017. doi: http://doi.org/10.1016/j.ijheatmasstransfer.2017.06.057.

[13] SHEWALKAR, A.G., DHOBLE, A.S., THAWKAR, V.P., "Review on cooling techniques and analysis methods of an electric vehicle motor", *Journal of Thermal Analysis and Calorimetry*, 2024. doi: http://doi.org/10.1007/s10973-024-13091-x.

[14] YAN, W.M., TENG, H.Y., LI, C.H., *et al*., "Electromagnetic field analysis and cooling system design for high power switched reluctance motor", *International Journal of Numerical Methods for Heat & Fluid Flow*, v. 29, n. 5, pp. 1756–1785, 2019. doi: http://doi.org/10.1108/HFF-08-2018-0450.

[15] GAI, Y., KIMIABEIGI, M., CHONG, Y.C., *et al*., "Cooling of automotive traction motors: Schemes, examples, and computation methods", *IEEE Transactions on Industrial Electronics*, v. 66, n. 3, pp. 1681–1692, 2018.

[16] GNANIAH, A.M., SEHAR, F.I.R.E., MANGALARAJ, A., *et al*., "Thermal analysis of modified segmented switched reluctance motor with aluminium metal matrix composite fins used in cooling fan applications", *Matéria (Rio de Janeiro*), v. 29, n. 2, pp. e20240075, 2024. doi: http://doi.org/10.1590/1517-7076-rmat-2024-0075.

[17] SUN, X., WAN, B., LEI, G., *et al*., "Multiobjective and multiphysics design optimization of a switched reluctance motor for electric vehicle applications", *IEEE Transactions on Energy Conversion*, v. 36, n. 4, pp. 3294–3304, 2021. doi: http://doi.org/10.1109/TEC.2021.3078547.

[18] VANSOMPEL, H., SERGEANT, P., "Extended end-winding cooling insert for high power density electric machines with concentrated windings", *IEEE Transactions on Energy Conversion*, v. 35, n. 2, pp. 948–955, 2019.

[19] ARBAB, N., WANG, W., LIN, C., *et al*., "Thermal modeling and analysis of a double-stator switched reluctance motor", *IEEE Transactions on Energy Conversion*, v. 30, n. 3, pp. 1209–1217, 2015. doi: http://doi.org/10.1109/TEC.2015.2424400.

[20] EVANGELINE, S.I., DARWIN, S., RAJ, E.F.I., "A deep residual neural network model for synchronous motor fault diagnostics", *Applied Soft Computing*, v. 160, n. 111683, pp. 111683, 2024. doi: http://doi.org/10.1016/j.asoc.2024.111683.

[21] GUNDABATTINI, E., MYSTKOWSKI, A., IDZKOWSKI, A., *et al*., "Thermal mapping of a high-speed electric motor used for traction applications and analysis of various cooling methods: a review", *Energies*, v. 14, n. 5, pp. 1472, 2021. doi: http://doi.org/10.3390/en14051472.

[22] SHRIVATSAAN, M.M., GB, N., PALKA, R., *et al*., "Performance analysis of electric motors, comparing lightweight techniques and cooling methods: a review", *Proceedings of the Institution of Mechanical Engineers, Part C: Journal of Mechanical Engineering Science*, v. 238, n. 5, pp. 1732–1746, 2024. doi: http://doi.org/10.1177/09544062231181812.

[23] ELHOMDY, E., LIU, Z., LI, G., "Thermal and mechanical analysis of a 72/48 switched reluctance motor for low-speed direct-drive mining applications", *Applied Sciences (Basel, Switzerland)*, v. 9, n. 13, pp. 2722, 2019. doi: http://doi.org/10.3390/app9132722.

[24] NASAB, P.S., MOALLEM, M., CHAHARSOGHI, E.S., *et al*., "Predicting temperature profile on the surface of a switched reluctance motor using a fast and accurate magneto-thermal model", *IEEE Transactions on Energy Conversion*, v. 35, n. 3, pp. 1394–1401, 2020.

[25] JANG, J.H., CHIU, H.C., YAN, W.M., *et al*., "Numerical study on electromagnetics and thermal cooling of a switched reluctance motor", *Case Studies in Thermal Engineering*, v. 6, pp. 16–27, 2015.

[26] RAHNAMAEI, S.R., NEJAD, S.M.S., RASHIDI, A., *et al*., "Dynamic thermal model for winding temperature of an SRM in an integrated battery charger utilized in electric vehicles", *IEEE Transactions on Energy Conversion*, v. 36, n. 3, pp. 1766–1775, 2020.

[27] GAN, C., CHEN, Y., CUI, X., *et al*., "Comprehensive investigation of loss calculation and sequential iterative fluid-solid coupling schemes for high-speed switched reluctance motors", *IEEE Transactions on Energy Conversion*, v. 36, n. 2, pp. 671–681, 2020.

[28] CHEN, H., WANG, K., YAN, W., *et al*., "Temperature analysis of switched reluctance motor based on equivalent heat circuit method", *IEEE Transactions on Applied Superconductivity*, v. 31, n. 8, pp. 1–4, 2021. doi: http://doi.org/10.1109/TASC.2021.3117753.

[29] JIA, S., QU, R., KONG, W., *et al*., "Stator/rotor slot and winding pole pair combinations of DC-biased current vernier reluctance machines", *IEEE Transactions on Industry Applications*, v. 54, n. 6, pp. 5967–5977, 2018. doi: http://doi.org/10.1109/TIA.2018.2859310.

[30] DIAO, K., SUN, X., LEI, G., *et al*., "System-level robust design optimization of a switched reluctance motor drive system considering multiple driving cycles", *IEEE Transactions on Energy Conversion*, v. 36, n. 1, pp. 348–357, 2020.

[31] ÇALIK, H., ÖZOĞLU, Y., UNDIL, S.H., *et al*., "A study on torque ripple improvement compared to a modified rotor and stator poles SRMs with classical SRMs using dynamic and FFT analysis", *Electric Power Components and Systems*, v. 51, n. 13, pp. 1328–1337, 2023.

[32] KUMAR, A., MARWAHA, S., MANNA, M., "Torque ripple mitigation of switched reluctance motor for water pumping applications at off-grid locations", *Journal of Engineering Science and Technology*, v. 18, n. 1, pp. 147–166, 2023.

[33] AJAMLOO, A.M., IBRAHIM, M.N., SERGEANT, P., "Design, modelling and optimization of a high power density axial flux SRM with reduced torque ripple for electric vehicles", *Machines*, v. 11, n. 7, pp. 759, 2023. doi: http://doi.org/10.3390/machines11070759.

[34] FANTIN IRUDAYA RAJ, E., APPADURAI, M., "Minimization of torque ripple and incremental of power factor in switched reluctance motor drive", In *Recent Trends in Communication and Intelligent Systems: Proceedings of ICRTCIS 2020*, pp. 125–133, 2021. doi: http://doi.org/10.1007/978-981-16-0167-5_14.

[35] COUSINEAU, J.E., BENNION, K., DEVOTO, D., *et al*., "Experimental characterization and modeling of thermal resistance of electric machine lamination stacks", *International Journal of Heat and Mass Transfer*, v. 129, pp. 152–159, 2019. doi: http://doi.org/10.1016/j.ijheatmasstransfer.2018.09.051.

[36] PRADHAN, S.K., SAHOO, M.R., RATHA, S., *et al*., "Graphene-incorporated aluminum with enhanced thermal and mechanical properties for solar heat collectors", *AIP Advances*, v. 10, n. 6, pp. 065016, 2020. doi: http://doi.org/10.1063/5.0008786.